Appl Phys A (2010) 99: 607–611
DOI 10.1007/s00339-010-5619-y

Applied Physics A
Materials Science & Processing

Investigation of the ϵ phase in the Fe–Al system by high-temperature neutron diffraction

Sven C. Vogel · Frank Stein · Martin Palm

Received: 15 April 2009 / Accepted: 24 February 2010 / Published online: 1 April 2010

Abstract In the central part of the Fe–Al system between about 58 and 65 at.% Al, a high-temperature phase denoted as ϵ occurs with a hitherto unknown crystallographic structure. The phase is stable between 1231°C and 1095°C. In order to study the crystallographic structure of the ϵ phase, in situ high-temperature neutron time-of-flight diffraction experiments have been performed at the HIPPO instrument at the Los Alamos Neutron Science Center (LANSCE). The ϵ phase was found to have the formula Fe_5Al_8 with a body-centred cubic structure of the Hume–Rothery Cu_5Zn_8 type ($I\bar{4}3m$ (No. 217), $Z = 4$, cI52) and 52 atoms in the unit cell. Its lattice parameter is $a = 8.9756(2)$ Å at 1120°C, which is 3.02 times that of cubic FeAl (B2) at the same temperature. We report here the evolution of the crystallographic parameters over the temperature range between 1080°C and 1120°C.

1 Introduction

The iron–aluminum system is of considerable commercial interest for structural applications. The existence of an intermetallic, high-temperature phase in the Fe–Al system at around 60 at.% Al is known since over a century [1]. However, since this phase is not quenchable and in situ X-ray diffraction work is hindered by rapid grain growth, attempts to solve the structure using X-rays in situ or on quenched samples were inconclusive [2, 3]. Adding ∼5 at.% Cr, Mo, or Ti as a third alloying element suppresses the eutectoid decomposition [4–6] and the retained structure was described with a rhombohedral Cr_5Al_8-type structure (space group R3m (160), Pearson symbol hR78, Strukturbericht designation $D8_{10}$) with lattice parameters of a = 12.70 Å and c = 7.90 Å. However, the question remains whether the binary ϵ phase has the same or a different crystal structure as the ternary phase. Consequently, the crystal structure of this phase was unknown until recently. Neutron diffraction, with a probed volume of ∼1 cm^3, overcomes grain growth problems as even with grains of the order of 1 mm in diameter more than 1000 grains are probed. The composition of interest for this work is around the eutectic composition of Fe-60Al. This material consists of cubic FeAl (B2) and triclinic $FeAl_2$ at room temperature. In a recent re-investigation of the Fe–Al phase diagram by differential thermal analysis [7], it was shown that the ϵ phase is formed at 1095°C followed by melting at 1231°C (see Fig. 1). The details of the crystal structure of the ϵ phase determined in this work are reported elsewhere [8] and here we report the evolution of the crystallographic parameters over the temperature range between 1080°C and 1120°C as well as details of the Rietveld analysis.

2 Sample preparation & characterization

About 200 g of an alloy of nominal composition Fe-60 at.% Al has been produced from Fe (purity 99.95 wt.%) and Al (99.999 wt.%) by crucible-free levitation melting. After melting, the alloy was drop-cast into a cold copper mould of 22 mm in diameter. Slices were cut from ingot by electro-discharge machining (EDM). The material was characterized by metallography, XRD, electron probe microanalysis

S.C. Vogel (✉)
Los Alamos Neutron Science Center, Los Alamos, NM 87545, USA
e-mail: sven@lanl.gov

F. Stein · M. Palm
Max-Planck-Institut für Eisenforschung GmbH, Düsseldorf, Germany

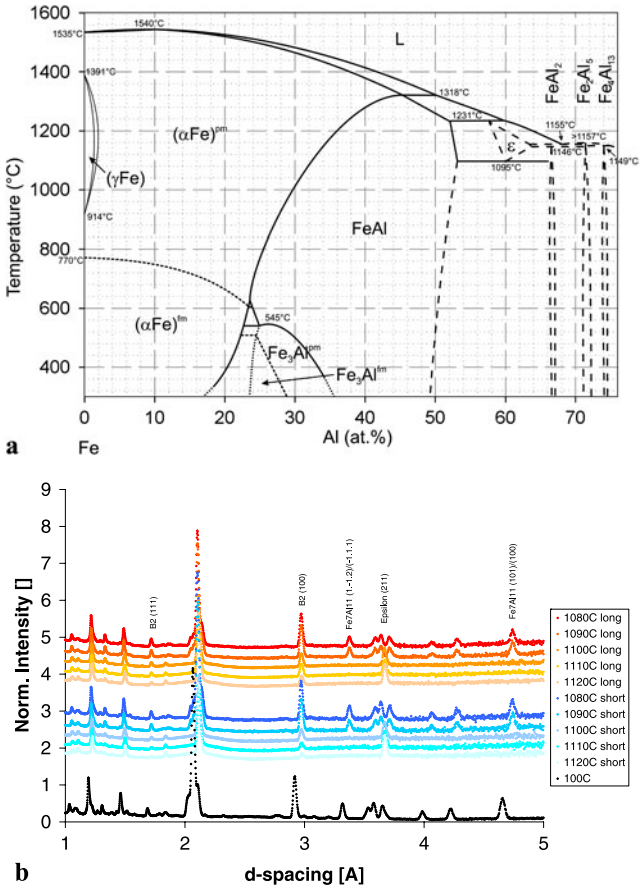

Fig. 1 (**a**) Fe–Al phase diagram [7]. (**b**) Overview of the measured data

(EPMA) and DTA and the results can be found elsewhere [7, 8]. A cylindrical sample of 7 mm in height and 9 mm in diameter was cut from the as-cast material, still containing ∼1000 grains should grain growth to a grain size of 1 mm occur.

3 Experiments & results

In order to investigate the formation and decomposition of the ϵ phase, high-temperature neutron time-of-flight diffraction experiments were performed at the Los Alamos Neutron Science Center (LANSCE) on the HIPPO (High-Pressure-Preferred Orientation) instrument allowing combined crystal structure and texture measurements at temperatures up to 1150°C [9, 10]. 26 out of the 50 HIPPO detector panels are usable with the furnace covering nominal diffraction angles of 140°, 90°, and 40°. The vanadium heating elements and heat shields of the ILL-type furnace were utilized for this experiment. The sample was placed in a vanadium sample holder and heated in vacuum ($<10^{-5}$ Torr). Measurements were performed in different orientations by rotating the sample on the vertical axis by 0°, 45°, 67.5°, and 90° and measuring for 15 minutes in each orientation in order to allow for the detection of possibly existing texture effects [11] (at 100°C integration times were ∼30 minutes/orientation). The high-temperature measurement was repeated with 30 minutes count time per orientation to verify reproducibility (see Fig. 1b). We found excellent reproducibility within statistical uncertainties and therefore report only the results from the 30 minutes/orientation runs. The sample position for the neutron time-of-flight experiment at 100°C was refined using the B2 lattice parameter obtained from the room temperature (25°C) X-ray measurement corrected for thermal expansion with a coefficient of thermal expansion of 18.0×10^{-6} C^{-1} [12, 13] to 2.9136 Å, ensuring reliable absolute lattice parameters at high temperature. FeAl has an ordered bcc structure (CsCl/B2 structure type, space group $Pm\bar{3}m$, Pearson symbol cP2). For the $FeAl_2$ phase we used the triclinic structure (space group P1, Pearson symbol aP18) determined by Corby and Black [14].

The initial texture refinement yielded a very mild texture for all runs and for the subsequent structure analysis using the GSAS software package [15], the four orientations measured for texture analysis were integrated (smoothing out further the weak existing preferred orientation) and the structural parameters were then refined simultaneously against the backscattering 140° and 90° banks over d-spacing ranges of 0.6 Å to 5 Å. A combined texture and crystal structure refinement for each temperature was also attempted, but resulted in larger uncertainties for the structural parameters and a negligible preferred orientation. Therefore, the integration of full rings and several sample orientations provides sufficient averaging of the preferred orientations to assume a random texture at the benefit of greatly improved counting statistics. For the dataset obtained at 100°C, the B2 lattice parameter was fixed and used to refine the linear time-of-flight to d-spacing conversion parameters DIFC for both banks, calibrating essentially the sample position. The DIFC parameters were kept fixed in subsequent refinements. The phase scale factors for each of the phases for both histograms were constrained together to provide identical weight fractions for both histograms. Linear absorption parameters were refined for both histograms, mostly to adjust for an overestimation of the incident neutron intensity due to air scatter contributions. The lattice parameters for the $FeAl_2$ phase were refined together with peak profile parameters σ_1 for each phase and histogram. The number of observations was not deemed sufficient to refine the thermal motion parameters of all 18 atoms of the $FeAl_2$ structure (3 shared sites), so the thermal motion parameters of atoms of the same species were constrained together to stabilize the refinement. The refinement of the thermal motion parameter for the Al atoms in $FeAl_2$ was still instable and we further constrained this parameter with the thermal motion parameter of the Al atom in FeAl (B2) phase. The reason for this

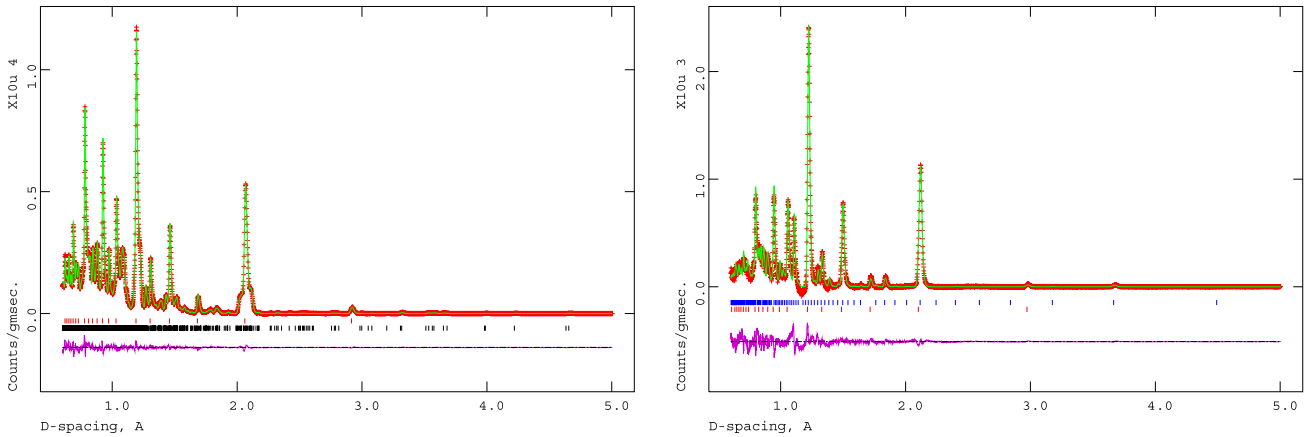

Fig. 2 Data from the 90° detectors (*crosses*) at 100°C (*left*) and 1120°C (*right*) with Rietveld refinements (*line through the data points*) and *difference curve* (below the data). The *tickmarks* indicate calculated peak positions of the $FeAl_2$ (*bottom row*, *left dataset*), FeAl (*top row*, *left dataset*, and *bottom row*, *right dataset*), and ϵ (*top row*, *right dataset*) phases. The background is subtracted for clarity

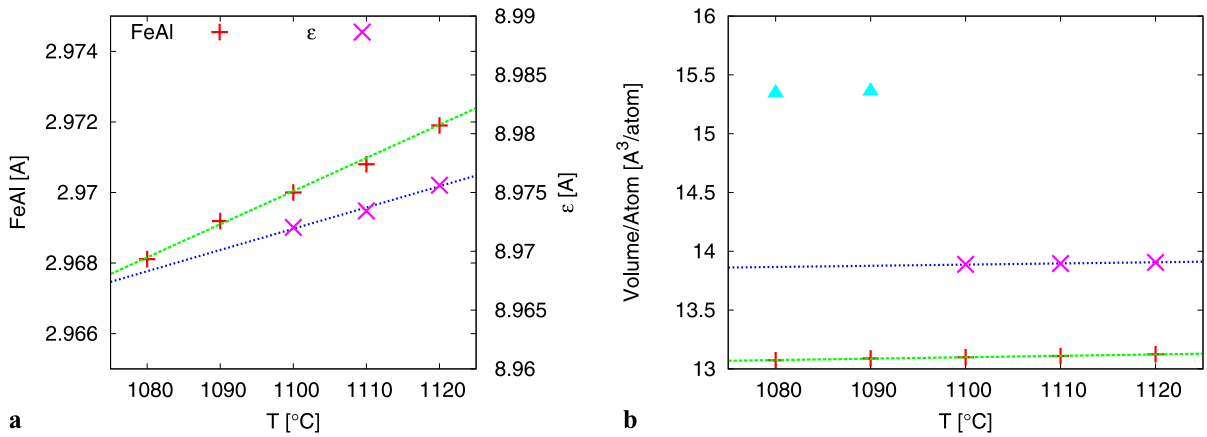

Fig. 3 (**a**) Lattice parameters of the cubic phases. (**b**) Volume per atom for the high-temperature runs ('+' FeAl, '×' ϵ, *triangles* $FeAl_2$)

Table 1 Weight fractions and unit cell volumes from Rietveld refinements

T [°C]	Weight fraction [%]			V [Å^3]		
	B2	ϵ	$FeAl_2$	B2	ϵ	$FeAl_2$
100	41.7(2)		58.3	24.734		262.48(2)
1080	49.6(3)		50.4	26.148(1)		276.21(2)
1090	49.9(3)		50.1	26.177(1)		276.49(2)
1100	33.5(4)	66.5		26.198(2)	722.22(5)	
1110	39.3(4)	60.7		26.219(2)	722.56(6)	
1120	23.3(4)	76.7		26.249(3)	723.09(5)	

is likely the weak neutron scattering power of the Al atoms compared to the Fe atoms. The site-occupation factors for the shared Al/Fe positions were also refined (constrained to a sum of 1 per site) together with the atom positions of all 21 atoms. Since the main purpose of this paper is the structure of the ϵ phase, we omit the results here. The refinements of the high-temperature runs were started with the 100°C refinement. Besides fixing DIFC and replacing the histograms, the initial values for the lattice parameters were adjusted for the thermal expansion. The total number of parameters for the 100°C, 1080°C, and 1090°C runs were 107. For the runs at 1100°C and above, no $FeAl_2$ was detected and this phase was replaced by the ϵ phase, but the same parameter set was refined. Examples of Rietveld refinements are shown

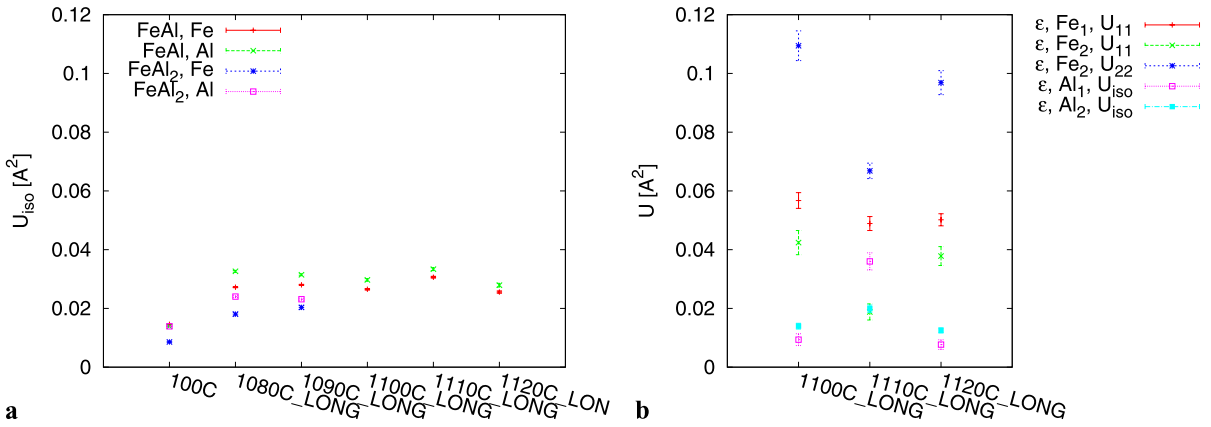

Fig. 4 Thermal motion parameters of the $FeAl_2$ and FeAl (**a**), as well as ϵ (**b**) phases with their uncertainties

Table 2 Atom positions (times 10,000) for the atoms of the ϵ phase

T [°C]	x_{Fe1}	x_{Al1}	x_{Fe2}	x_{Al2}	z_{Al2}
1100	8308(7)	1366(7)	3558(8)	3130(6)	133(7)
1110	8334(5)	1188(9)	3601(7)	3149(10)	216(8)
1120	8293(6)	1364(5)	3534(6)	3140(5)	140(6)

in Fig. 2. The weight fractions and unit cell volumes resulting from the Rietveld refinements are listed in Table 1 with the lattice parameters of the two cubic phases and the volume per atom shown in Fig. 3. Thermal motion parameters are shown in Fig. 4 with the atom positions for the ϵ phase listed in Table 2.

4 Discussion

The Rietveld fits show generally good agreement with the data. There are no indications of additional phases. At 1080°C and above, we observed significant diffuse scattering, manifested in oscillations in the difference curve. We were not successful in using the GSAS models for diffuse scattering with the Fe–Al, Fe–Fe, and Al–Al atom distances derived from the crystalline structure and therefore increased the number of background coefficients from 16 to 20 and 24 for the 140° and 90°, respectively (Chebyschef polynomial of the first kind, GSAS background function type 1). The origin of the diffuse scattering is likely caused by positional disorder due to the proximity to the melting temperature. However, even at 100°C we observed some diffuse scattering, resulting in the relatively large number of 16 background (compared to typically 8 for other materials). This may be explained by substitutional disorder of the Fe and Al atoms.

The presence of the ϵ phase at 1100°C and above and its absence at 1090°C is in agreement with the transition temperature of 1095°C determined by Stein et al. [7], but does not match the transition temperature of 1102°C reported by Kattner and Burton [16]. We note that the specific volumes and cubic lattice parameters increase almost linearly with temperature, for the B2 phase even across the transition temperature (Fig. 2(b)). The linear coefficients of thermal expansion for FeAl (B2) and ϵ from the high-temperature runs with a reference temperature of 1100°C are $\alpha = 31(2) \times 10^{-6}$ °C^{-1} and $\alpha = 20(2) \times 10^{-6}$ °C^{-1}, respectively. For FeAl (B2), Porter and Mazias report 24.3×10^{-6} °C^{-1} for an alloy with 35.8 at.% Al [12], whereas Reddy and Deevi report $24.3 \pm 0.5 \times 10^{-6}$ °C^{-1} [13]. The thermal motion parameters also increase more than twofold from 100°C to 1080°C and above as expected. While the structural parameters and weight fractions for the 1100°C and 1120°C datasets agree well, the results for the 1110°C dataset produce outlayers for the weight fractions and thermal motion parameters that are outside the error bars of these parameters. The reason for this is not understood, but the effect persists even when this dataset is refined starting from the 1100°C or 1120°C datasets or with varied refinement strategies (different parameter turn-on sequence). Further investigations are required to solve this issue. It is peculiar that the FeAl (B2) thermal motion parameters for both Al and Fe atoms seem to drop from 1080°C to 1120°C, which is counter-intuitive with increasing temperature. The biggest problem with these datasets, however, are the thermal motion parameters of the ϵ phase. The magnitudes of the thermal motion parameters in particular of the Fe atoms, which have much more neutron scattering power than the Al atoms and therefore should be determined more reliably, are much too large when compared with corresponding the FeAl (B2) and $FeAl_2$ values. We attempted several different refinement strategies, including initially constraining parameter values together or using isotropic instead of anisotropic representation of the thermal motion, but in each case we obtained similar results. We also attempted to refine the site-occupation factors, resulting in either values around 1 (e.g. a site fully

occupied by one element only) or unphysical values (e.g. a total occupation by more than one atom per site), making mixed occupation of the four crystallographic sites in the determined ϵ crystal structure unlikely. The atom positions of the ϵ phase and therefore bond-lengths and angles are only mildly affected by these concerns.

5 Conclusion

A century after the discovery of the ϵ phase in the Fe-Al system, we believe our work determines the crystal structure of this phase to be of the cubic Cu_5Zn_8 type (γ_1 brass structure, for a discussion of this structure see e.g. [17]) with a lattice parameter of $a = 8.9756(2)$ Å at 1120°C, which is 3.02 times that of cubic FeAl (B2) at the same temperature. The ϵ phase should be therefore designated Fe_5Al_8 from now on. Neutron diffraction turned out to be a crucial tool for this structure determination due to the problems for other diffraction techniques arising from grain growth. Further research is required to confirm and understand the very large values obtained for the thermal motion parameters of the Fe_5Al_8 phase.

Acknowledgements This work has benefited from the use of the Lujan Center at Los Alamos Neutron Science Center, funded by DOE Office of Basic Energy Sciences and Los Alamos National Laboratory funded by Department of Energy under contract W-7405-ENG-36.

References

1. A.G.C. Gwyer, Z. Anorg. Chem. **57**, 113–153 (1908)
2. A. Osawa, Sci. Rep. Tohoku Univ. **22**, 803–823 (1933)
3. A. Taylor, R.M. Jones, J. Phys. Chem. Solids **6**, 16–37 (1958)
4. M. Palm, J. Alloys Compd. **252**, 192–200 (1997)
5. R. Ducher, F. Stein, B. Viguier, M. Palm, J. Lacaze, Z. Metallkd. **94**, 396–410 (2003)
6. M. Eumann, G. Sauthoff, M. Palm, Intermetallics **16**, 834–846 (2008)
7. F. Stein, M. Palm, Int. J. Mater. Sci. **98**, 580–588 (2007)
8. F. Stein, S.C. Vogel, M. Eumann, M. Palm, Intermetallics **18**, 150–156 (2010)
9. H.-R. Wenk, L. Lutterotti, S. Vogel, Nucl. Instrum. Methods Phys. Res. A **515**(3), 575–588 (2003)
10. S. Vogel, C. Hartig, L. Lutterotti, R.B. von Dreele, H.-R. Wenk, D.J. Williams, Powder Diffr. **19**, 65–68 (2004)
11. S. Matthies, J. Pehl, H.-R. Wenk, L. Lutterotti, S. Vogel, J. Appl. Crystallogr. **38**, 462–475 (2005)
12. W.D. Porter, P.J. Maziasz, Scr. Metall. Mater. **29**, 1043–1048 (1993)
13. B.V. Reddy, S.C. Deevi, Intermetallics **8**, 1369–1376 (2000)
14. R.N. Corby, P.J. Black, Acta Crystalogr. B **29**, 2669–2677 (1973)
15. A.C. Larson, R.B. von Dreele, Los Alamos National Laboratory Report LAUR 86-748 (2004)
16. U.R. Kattner, B.P. Burton, in: *Phase Diagrams of Binary Iron Alloys*, ed. by Okamoto, H., ASM International, Materials Park, OH (1993), p. 12
17. O. Gourdon, D. Gout, D.J. Williams, T. Proffen, S. Hobbs, G.J. Miller, Inorg. Chem. **46**, 251 (2007)